

DOI: 10.1002/chem.201300334

Novel Functionalized Microporous Organic Networks Based on Triphenylphosphine

Qiang Zhang,^[a, b] Yanqin Yang,^[a, b] and Suobo Zhang*^[a]

Abstract: This article describes the synthesis and functions of phosphine or phosphine oxide functionalized networks (PP-P or PP-PO; PP=porous polymer). These materials were predominantly microporous and exhibited high surface areas (S_{BET} : 1284 and 1353 m^2g^{-1} for PP-P and PP-PO, respectively), with high CO_2 (2.46 and 3.83 mmol g^{-1} for PP-P and PP-PO, respectively) uptake capacities. Pd

nanoparticles can be simply incorporated into the functionalized networks (PP-P-Pd or PP-PO-Pd) through a facile one-step impregnation. A yield of 98% was obtained in the Suzuki reaction between 1-chlorobenzene and *p*-

tolylboronic acid with the PP-P-Pd system, which was higher than that obtained when PP-PO-Pd (53.2%) or $[\text{Pd}(\text{PPh}_3)_4]$ (38.2%) was used as the catalyst. The superior catalytic ability of PP-P-Pd can be attributed to the structural features that incorporate triarylphosphine within a microporous structure.

Keywords: carbon storage • heterogeneous catalysis • microporous materials • nanoparticles • phosphines

Introduction

The synthesis and application of microporous organic polymers (MOPs) has recently spurred scientific interest within the fast developing field of material science.^[1] Their most prominent feature of high intrinsic levels of porosity along with diverse and simple chemical routes available for their synthesis makes these materials attractive candidates for a variety of applications in areas such as molecular separations, heterogeneous catalysis, and gas storage.^[1] MOPs can be distinguished, according to recent reports, into 1) microporous polymer networks, such as the well-described hypercross-linked resins,^[2] 2) a class of porous covalent organic framework,^[3] 3) conjugated microporous polymers,^[4] and 4) polymers with intrinsic microporosity (PIMs).^[5] Microporous polymer networks represent a family of robust porous organic polymer networks with high BET surface areas that can exceed 1000 m^2g^{-1} .^[6] Unlike solution-processable PIMs, the permanent porosity in microporous polymer networks is the result of extensive crosslinking reactions that prevent the polymer chains from collapsing into a dense, nonporous

state.^[7] Among other features, microporous polymer networks possess robustness and scalability, the materials have good thermal and excellent chemical stability (e.g., in the presence of strong acids and bases), and can be readily produced on a large scale. Such materials have been used as sorbents for organic vapors,^[7] for the recovery of organic compounds from water,^[8] and in heterogeneous catalytic systems.^[9]

Most of the microporous polymer networks synthesized to date have been produced as intractable solids and their chemical functionalization was therefore limited.^[6,10] The development of porous materials containing functional groups to fulfill a certain task is a pertinent requirement.^[7-9] Functionalization of microporous polymers could open up second-generation porous materials with useful combined chemical and physical properties.^[1c,4b,11] Recently, many microporous organic polymers containing functional units such as bipyridine, metalloporphyrin, and triazine rings, have been reported.^[12] These materials exhibit excellent properties such as superior catalytic activity and high CO_2 uptake capacity.^[12]

The construction of carbon-carbon and carbon-heteroatom bonds by transition-metal-mediated organic processes has become fundamental to the science of synthetic organic chemistry in the past decades. In modern organic synthesis, triphenylphosphine is an important ligand to noble metals in carbon-carbon and carbon-heteroatom cross-coupling reaction systems, for example, in the Wittig reaction,^[13] the Mitsunobu reaction,^[14] the Suzuki-Miyaura cross-coupling reaction,^[15] Mukaiyama-Corey lactonization,^[16] the Appel reaction,^[17] and the Staudinger reaction.^[18] Although homogeneous catalysts have been extensively investigated, their practical applications on a large scale remain challenging because the catalysts are expensive and it is difficult to recover the

[a] Dr. Q. Zhang,* Dr. Y. Yang,* Prof. S. Zhang
Key Laboratory of Polymer Ecomaterials
Changchun Institute of Applied Chemistry
Chinese Academy of Science
Changchun 130022 (P.R. China)
Fax: (+86)430-85272117
E-mail: sbzhang@ciac.jl.cn

[b] Dr. Q. Zhang,* Dr. Y. Yang*
Graduate School of Chinese Academy of Science
Beijing 100049 (P.R. China)

[*] These authors contributed equally to this work.

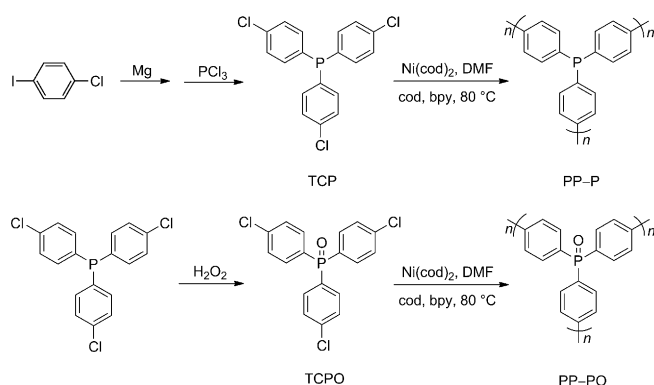
Supporting information for this article is available on the WWW under <http://dx.doi.org/10.1002/chem.201300334>.

metal from the product. One approach that has been used to address this issue of separation of the catalyst is to heterogenize the metal catalyst by attaching it to a solid support. A number of solid materials, such as carbon structures,^[19] polymers,^[20] mesoporous silica,^[21] and zeolites^[22] have been employed as supports for catalysts. Unfortunately, heterogenizing the catalyst on a solid support often results in decreased activity.^[23] Recently, microporous polymer networks have emerged as a new class of attractive functional materials.^[12a,24] Due to their extraordinarily high surface area and well-defined pore structure, microporous polymer networks can be used as supports for catalytic systems.

In the present work, a porous polymer network with trivalent phosphorus atoms as aromatic ring linkers (PP-P) was synthesized by the homocoupling of tris(4-chlorophenyl)phosphine. The material exhibits a high surface area of 1284 m² g⁻¹ in the BET model and 1970 m² g⁻¹ in the Langmuir model. To the best of our knowledge, this is the first report of a microporous organic polymer based on triphenylphosphine unit. Palladium nanoparticles supported on PP-P have been prepared that exhibited extremely good catalytic activity for Suzuki reactions. To investigate the role of the trivalent P atoms in the catalytic ability of PP-P-Pd, the porous polymer network with phosphine oxide as aromatic ring linkers (PP-PO) was also synthesized.

Results and Discussion

Initially, two monomers were synthesized, as shown in Scheme 1. The polymer networks were synthesized from



Scheme 1. Synthesis of monomers and microporous polymers. TCP = tris(4-chlorophenyl)phosphine, TCPO = tris(4-chlorophenyl)phosphine oxide, cod = 1,5-cyclooctadiene, bpy = 2,2'-bipyridine.

these monomers through the Yamamoto reaction route. These reactions produced off-white powdery compounds, had a low density, and were not soluble in any common organic solvent. For purification, the sample was successively immersed in water, ethanol, chloroform, and propan-2-one to remove solvent residues and starting materials, and was finally heated at 120 °C for 12 h in vacuum to remove volatile entities. The polymerization process was monitored by

FTIR analysis, whereby the disappearance of the C–Cl ($\tilde{\nu}$ = 750 cm⁻¹) vibrations of the starting material indicated both the complete consumption of monomers and the success of phenyl–phenyl coupling (see Figure S1 in the Supporting Information).

The PP-P polymer was characterized by ³¹P solid-state NMR analysis (Figure S2a). A signal at δ = -9.2 ppm was observed, corresponding to phosphorus in triphenylphosphine units, and a signal at δ = 25.2 ppm was assigned to phosphorus in phosphine oxide units, which results from aerobic oxidation of P^{III}. The integration ratio of signals (phosphine oxide to phosphine atoms) was close to 1:20. In the ³¹P solid-state NMR spectrum of PP-PO (Figure S2b), only a single peak was observed at δ = 24.7 ppm, which was assigned to P^V. Similar to other microporous polymers,^[6] the scanning electron micrograph revealed that samples are composed of loose agglomerates of small particles with diameters of approximately 200 nm (Figure S3). The polymers were also stable towards water, base, and acid; indeed no change in surface area was observed even after the material was treated with 10 M HCl. Thermal gravimetric analysis (TGA) indicated that the polymer networks remained stable up to 500 °C (Figure S4).

Nitrogen adsorption–desorption isotherm measurements can be used to analyze the porous properties of microporous polymers.^[25,26] PP-P and PP-PO possess similar nitrogen adsorption–desorption isotherms, which are combinations of type I and II nitrogen sorption isotherms (Figure 1a) according to IUPAC classification.^[27] The high uptake at very low pressures (0–0.1 bar) indicates a high microporosity.^[20,28] With increasing pressure, the nitrogen uptake increased slightly, which indicates a little external surface area due to the presence of very small particles.^[20] These results suggest that PP-P and PP-PO have a predominantly microporous structure in their framework.^[27] Using a conventional flask procedure, BET specific surface areas of 1284 m² g⁻¹ for PP-P and 1353 m² g⁻¹ for PP-PO were obtained (Table 1).

Table 1. Porosity properties of microporous polymers.

Polymer	S_{BET} [m ² g ⁻¹] ^[a]	S_{Lang} [m ² g ⁻¹]	V [cm ³ g ⁻¹] ^[b]	V_{M} [cm ³ g ⁻¹] ^[c]
PP-P	1284	1970	1.11	0.57
PP-PO	1353	2046	1.07	0.72

[a] Specific surface area calculated from the nitrogen adsorption isotherm by using the BET method. [b] Total pore volume at P/P_0 = 0.97. [c] Micropore volume calculated from the nitrogen adsorption isotherm by using the t-plot method.

The pore size calculated from nonlinear density functional theory (NLDFT) gave a value of approximately 1.6 nm for PP-P and 1.5 nm for PP-PO (Figure 1b). Recently, Cooper and co-workers reported a series of nitrogen-containing microporous polymers based on poly(triethynylphenyl)amine,^[29] their material exhibited BET specific surface areas in the range 500–1100 m² g⁻¹, which are a little lower than those of our system. This result stems from two factors: dif-

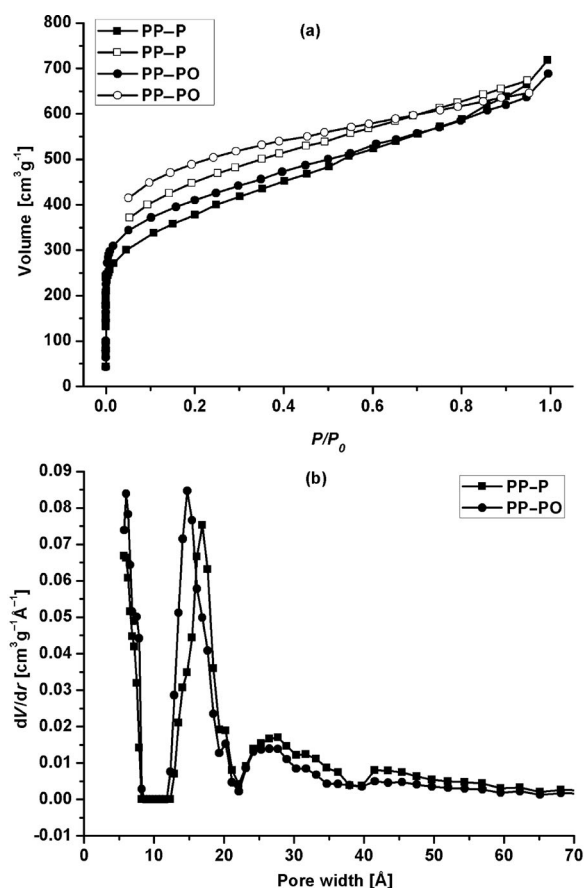


Figure 1. a) Nitrogen adsorption–desorption isotherms of microporous polymer networks measured at 77 K. b) Pore-size distribution of microporous polymer networks (adsorption and desorption branches are labeled with filled and open symbols, respectively).

ferent central link atoms (nitrogen and phosphine) and monomer strut length.

Adsorption processes for CO₂ capture are essential today in the context of mitigating the problems caused by global warming from the emission of greenhouse gases.^[30] Adsorption on porous solid media using pressure and/or temperature swing approaches is an emerging alternative that should help to reduce the costs associated with the capture step. The regeneration energy required for CO₂ capture using dry solid sorbent is significantly reduced, compared with aqueous amine-based process.^[31] For solid sorbents to be competitive with existing amine-based scrubbing systems, the CO₂ adsorption capacity must be in the range of 3–4 mmol g⁻¹ of sorbent.^[32] The PP-PO network showed high volumetric CO₂ uptake of 3.83 mmol g⁻¹ (1 bar and 273 K), and the P-functionalized networks adsorbed less CO₂ (2.46 mmol g⁻¹), despite exhibiting similar surface areas (Figure 2). The correlation between CO₂ uptake and the surface area is not proportional, and chemical functionality also plays a role.^[26,32,33] For our system, the phosphine oxide groups in PP-PO may involve stronger interactions with CO₂ molecules than trivalent phosphorus and enhance CO₂ adsorption capacity. As a comparison of the adsorption effi-

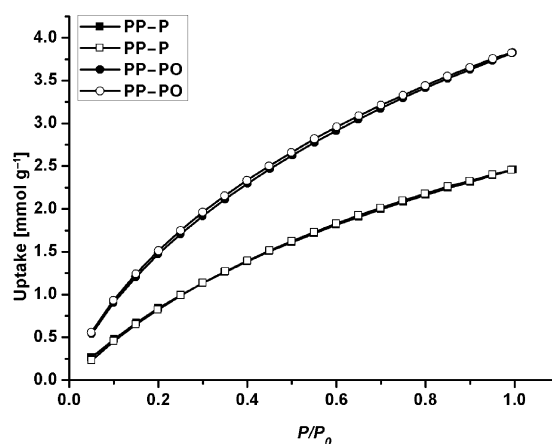


Figure 2. CO₂ adsorption (closed) and desorption (open) isotherms at 273 K.

ciency, BPL carbon ($S_{\text{BET}} = 1150 \text{ m}^2 \text{ g}^{-1}$; a common reference material for CO₂ uptake) exhibited an uptake of 1.9 mmol g⁻¹ at 1 bar and 273 K.^[34] As an additional reference, the covalent organic framework, COF-102 ($S_{\text{BET}} = 3620 \text{ m}^2 \text{ g}^{-1}$) showed CO₂ uptake of 1.56 mmol g⁻¹ at 1 bar and 273 K.^[35]

Recently, microporous organic polymers with functional groups have been found to have a broad range of potential applications in heterogeneous catalyst systems due to their large permanent surface area.^[9b,36] In this work, because the PP-P polymer networks contain tertiary phosphines and have a large surface area, their application as catalytic systems attracted our interest. Generally, polymer-supported Pd catalysts have been obtained by using [Pd(PPh₃)₄] as a soluble Pd source.^[15,37]

We immobilized Pd nanoparticles on PP-P by a simple impregnation of PP-P with [Pd(PPh₃)₄] solution at room temperature. Determination of the Pd content was carried out by catalyst digestion followed by elemental analysis, and the results are shown in Table S1 (see the Supporting Information). The black solution lost all its color at a Pd/P molar ratio of 1:1, whereas the polymer networks became a dark black color. Inductively coupled plasma (ICP) analysis confirmed the loading of Pd on the PP-P to be 11.2 wt%, which corresponds to the complete absorption of Pd from the solution. The Pd content of the PP-P-Pd can be readily controlled through the [Pd(PPh₃)₄] feed.

Generally, X-ray photoelectron spectra (XPS) allow the valence and electron state change of atoms to be characterized. To investigate the coordination binding of Pd to the phosphine ligand of the polymer network, we used XPS to characterize the Pd valence state in PP-P-Pd and [Pd(PPh₃)₄]; the results are shown in Figure S5. It was found that the Pd in the polymer networks exhibited the same binding energy as that of [Pd(PPh₃)₄], which indicates the phosphine ligand of the polymer networks coordinate to Pd. Figure 3 shows the transmission electron microscopy images of PP-P-Pd; the TEM analysis confirms that the Pd⁰ particles were uniformly dispersed in the polymer networks, and

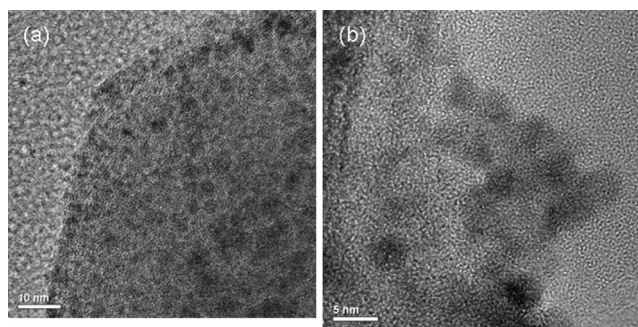


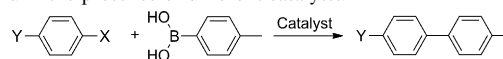
Figure 3. TEM images of PP-P-Pd. Scale bar: a) 10 nm and b) 5 nm.

that the average particle size was 3 nm. Larger Pd⁰ aggregates were not observed in PP-P-Pd, even when the weight ratio of Pd to the polymeric scaffold was increased to 14%. The crystal lattice of Pd⁰ was examined by high-resolution TEM (Figure 3b), and the interplanar spacing was found to be 0.27 nm. Generally, hypercrosslinked microporous polymers show a relatively broad pore size distribution. The pore size distribution of PP-P indicated the presence of micropores (1–2 nm) and mesopores (2–4 nm), with the larger Pd particles occupying the latter. Pd atoms in a nonaggregation state in the micropores were also detected by TEM-EDX in PP-P-Pd (Figure S6). The BET surface area decreased from 1248 m²g⁻¹ (PP-P) to 860 m²g⁻¹ (PP-P-Pd: 9.8%) (Figure S7a), but no significant change in the pore size was observed (Figure S7b).

As a model, we carried out Suzuki cross-coupling reactions to evaluate the catalytic ability and recyclability of the PP-P-Pd catalyst. To investigate the role of the oxidation state of the P atom in the catalytic ability of PP-P, PP-PO-Pd was also prepared. Due to environmental, economic, and safety concerns, the Suzuki reactions were performed in water with a suitable amount of EtOH used as a cosolvent to increase the solubility of the substrates. The cross-coupling reactions were carried out with 1 mol% Pd catalyst in H₂O/EtOH (3:1 v/v) at 80°C. When the reaction was complete, the reaction mass was extracted with diethyl ether (10 mL), and the yield of the product was determined by GC-MS analysis of the organic phase with dodecane as the internal standard.

As shown in Table 2, aryl iodides and bromides provided the cross-coupling products in more than 99% yield. Using both electron-rich and electron-deficient aryl chlorides with the PP-P-Pd system, the desired coupling products were obtained in high yields (more than 98%). This is significant, because aryl chlorides are known to be sluggish coupling partners.^[35] The coupling yields for aryl chlorides, with some recently reported catalytic systems based on Pd from other groups as well as ours, were about 30%.^[35] For comparison, when the cross-coupling reaction between 1-chlorobenzene and *p*-tolylboronic acid was carried out with [Pd(PPh₃)₄] under the same conditions, a yield of 38.2% was obtained. On the other hand, when the Pd nanoparticles were incorporated on PP-PO containing P^V, the material showed a

Table 2. Suzuki cross-coupling reactions of aryl halides with phenylboronic acid in the presence of different catalysts.



Entry	X	Y	Catalyst	Yield [%]
1	I	H	PP-P-Pd	99.9
2	Br	H	PP-P-Pd	99.1
3	Cl	H	PP-P-Pd	98.9
4	Cl	H	PP-PO-Pd	53.2
5	Cl	H	[Pd(PPh ₃) ₄]	38.2
6	Cl	CH ₃	PP-P-Pd	98.6
7	Cl	CHO	PP-P-Pd	99.0
8	F	H	PP-P-Pd	64.5

lower activity (yield: 53.2%) compared with PP-P-Pd for the coupling of 1-chlorobenzene and *p*-tolylboronic acid under the same conditions (Table 2, entry 4). This result indicates that the triarylphosphine improved the catalytic ability of PP-P-Pd.

Most gratifyingly, when PP-P-Pd was used as a catalyst for the reaction between fluorobenzene and *p*-tolylboronic acid, the coupling product was obtained in 64.5% yield. In general, catalytic C–C cross-coupling reactions of fluoro-derivatives are rare because of the strong C–F bond.^[36] This superior catalytic performance of PP-P-Pd is presumably due to the structural features that allow incorporation of the triarylphosphine inside the microporous structure. The reagents can be adsorbed into the porous channels by capillary condensation of the micropores where the catalyst particles are located. The concentration of reagents around the Pd nanoparticles is higher than that in the bulk solution. The small pore size (less than 2 nm) imposes a space confinement effect on the reactants, leading to a high catalytic activity. In addition, the triarylphosphine coordinated to the active palladium sites had a profound influence on the catalytic activity and stability of Pd⁰.^[37] It is well-known that triphenylphosphine-palladium complexes are widely used for coupling reactions due to their excellent catalytic activity.^[38]

For the practical application of a heterogeneous catalytic system, its stability and reusability are important factors. For metal-catalyzed reactions, including those involving palladium, leaching of the noble metal is a major cause of catalyst deterioration.^[36] In this work, we have also examined the recyclability and reusability of the PP-P-Pd catalyst. The PP-P-Pd was readily recovered from the reaction mixtures through simple filtration. The catalytic activity of the recovered PP-P-Pd catalyst proved to be almost constant, with the yield remaining within the range 99.1–97.2% after five consecutive runs (Table S2). The filtrate was analyzed by ICP-MS to estimate the palladium content and the results revealed that approximately 31 ppb of palladium leached into the solution, corresponding to an original metal loss of 0.005%, which is fifty times lower than the corresponding value (0.27%) reported for Kato's system.^[36] No change in the chemical structure of the PP-P polymer was detected by ³¹P solid-state NMR analysis after treatment with H₂O/EtOH (3:1 v/v) at 80°C for 100 h, which indicates that the

polymer networks possess excellent stability. Thus, all the evidence demonstrates the durability of the PP–P–Pd catalyst.

Conclusion

Phosphine and phosphine oxide functionalized microporous organic networks were prepared by using Yamamoto type cross-coupling reaction. The polymeric networks remained stable up to 500 °C and were also stable towards water, base, and acid. The networks exhibited large surface areas (S_{BET} : 1284 and 1353 m²g⁻¹ for PP–P and PP–PO, respectively), with high CO₂ (2.46 and 3.83 mmolg⁻¹ for PP–P and PP–PO, respectively) uptake capacities. Pd nanoparticles were incorporated into PP–P, which were uniformly dispersed in the polymer networks. The average particle size was found to be 3 nm, and the interplanar spacing was approximately 0.27 nm. The coupling reactions between aryl chlorides and *p*-tolylboronic acid gave the desired product in more than 98% conversion in the presence of PP–P–Pd. The superior catalytic performance of PP–P–Pd resulted from the unique structural features that incorporate the triarylphosphine inside the microporous structure.

Experimental Section

General methods: Solution-state ¹H NMR spectra were recorded with a 600 MHz JEOL JNM-EX-270 spectrometer. Chemical shifts are reported in ppm downfield from SiMe₄. Solid-state NMR spectra were obtained with a Chemagnetics CMS-400 spectrometer. TGA was performed with a PU 4K (Rigaku) at a heating rate of 10 °C/min with N₂ as carrier gas. Size and morphology of the samples were observed under a field-emission scanning electron microscope (Hitachi S-4800). TEM was carried out with a Jeol JEM 2000EXII operating at 200 kV. Volumetric gas adsorption was performed with an Autosorb-1 instrument (Quantachrome). Nitrogen adsorption isotherms at 77 K were measured in liquid-nitrogen baths.

Polymerization for PP–P: typical procedure: [Ni(cod)₂] (2.25 g, 8.18 mmol) was added to a solution of 1,5-cyclooctadiene (1.05 mL, 8.32 mmol) and 2,2'-bipyridyl (1.28 g, 8.18 mmol) in anhydrous DMF (100 mL) and the mixture was heated at 80 °C for 30 min. Tris(4-bromophenyl)phosphine (0.779 g, 1.57 mmol) was added to the resulting solution at 80 °C, and the mixture was stirred at that temperature for 10 h. After cooling to RT, the mixture was stirred at that temperature for 10 h. After cooling to RT, concentrated HCl (5 M, 20 mL) was added to the solution. The solid obtained was filtered and the residue was successively washed with H₂O, EtOH, CHCl₃, and propan-2-one. The polymer was then dried in a vacuum oven at 120 °C (83% yield).

Syntheses of polymer-supported palladium catalyst: Small portions of [Pd(PPh₃)₄] were added at RT to a suspension of the polymer in anhydrous toluene under an argon atmosphere. The reaction mixture was degassed with argon and stirred at RT for 20 h. The resin was filtered under vacuum and washed three times with toluene and Et₂O. The catalyst was dried under vacuum for 20 h.

Suzuki reaction: typical procedure: *p*-Tolylboronic acid (0.163 g, 1.2 mmol), K₂CO₃ (0.346 g, 2.5 mmol), Pd catalyst (1 mol%), aryl halide (1.0 mmol), and H₂O/EtOH (10 mL; 3:1 v/v) as solvent were added to a screw-capped vial with a sidetube under argon. The mixture was stirred at 80 °C for 6 h and then cooled. The product was extracted from the reaction mixture with diethyl ether, and the organic phase was analyzed by GC-MS.

Acknowledgements

This research was financially supported by the National Basic Research Program of China (No. 2009CB623401 and 2012CB932802) and the National Science Foundation of China (No. 51133008, 50825302, and 51021003).

- [1] a) N. B. McKeown, P. M. Budd, *Chem. Soc. Rev.* **2006**, *35*, 675–683; b) R. E. Morris, P. S. Wheatley, *Angew. Chem.* **2008**, *120*, 5044–5059; *Angew. Chem. Int. Ed.* **2008**, *47*, 4966–4981; c) J. X. Jiang, C. Wang, A. Laybourn, T. Hasell, R. Clowes, Y. Z. Khimyak, J. Xiao, S. J. Higgins, D. J. Adams, A. I. Cooper, *Angew. Chem.* **2011**, *123*, 1104–1107; *Angew. Chem. Int. Ed.* **2011**, *50*, 1072–1075; d) M. W. Schneider, I. M. Oppel, M. Mastalerz, *Chem. Eur. J.* **2012**, *18*, 4156–4160.
- [2] a) M. P. Tsyurupa, V. A. Davankov, *React. Funct. Polym.* **2002**, *53*, 193–203; b) M. G. Schwab, A. Lennert, J. Pahnke, G. Jonschker, M. Koch, I. Senkovska, M. Rehahn, S. Kaskel, *J. Mater. Chem.* **2011**, *21*, 2131–2135; c) S. Y. Moon, J. S. Bae, E. Jeon, J. W. Park, *Angew. Chem.* **2010**, *122*, 9694–9698; *Angew. Chem. Int. Ed.* **2010**, *49*, 9504–9508; d) J. Schmidt, M. Werner, A. Thomas, *Macromolecules* **2009**, *42*, 4426–4429.
- [3] a) H. M. El-Kaderi, J. R. Hunt, J. L. Mendoza-Cortes, A. P. Cote, R. E. Taylor, M. O'Keeffe, O. M. Yaghi, *Science* **2007**, *316*, 268–272; b) E. L. Spitler, W. R. Dichtel, *Nat. Chem.* **2010**, *2*, 672–677; c) J. W. Colson, A. R. Woll, A. Mukherjee, M. P. Levendorf, E. L. Spitler, V. B. Shields, M. G. Spencer, J. Park, W. R. Dichtel, *Science* **2011**, *332*, 228–231.
- [4] a) J. X. Jiang, F. Su, A. Trewin, C. D. Wood, H. Niu, J. T. A. Jones, Y. Z. Khimyak, A. I. Cooper, *J. Am. Chem. Soc.* **2008**, *130*, 7710–7720; b) R. Dawson, D. J. Adams, A. I. Cooper, *Chem. Sci.* **2011**, *2*, 1173–1177.
- [5] a) P. M. Budd, B. S. Ghanem, S. Makhseed, N. B. McKeown, K. J. Msayib, C. E. Tattershall, *Chem. Commun.* **2004**, 230–231; b) N. Du, H. B. Park, G. P. Robertson, M. M. Dal-Cin, T. Visser, L. Scoles, M. D. Guiver, *Nat. Mater.* **2011**, *10*, 372–375; c) J. Weber, N. Du, M. D. Guiver, *Macromolecules* **2011**, *44*, 1763–1767.
- [6] a) B. Li, R. Gong, W. Wang, X. Huang, W. Zhang, H. Li, C. Hu, B. Tan, *Macromolecules* **2011**, *44*, 2410–2414; b) C. F. Martín, E. Stöckel, R. Clowes, D. J. Adams, A. I. Cooper, J. J. Pis, F. Rubiera, C. Pevida, *J. Mater. Chem.* **2011**, *21*, 5475–5483.
- [7] a) H. Ren, T. Ben, E. Wang, X. Jing, M. Xue, B. Liu, Y. Cui, S. Qiu, G. Zhu, *Chem. Commun.* **2010**, *46*, 291–293; b) X. Liu, Y. Xu, D. Jiang, *J. Am. Chem. Soc.* **2012**, *134*, 8738–8741.
- [8] a) A. Li, H. Sun, D. Tan, W. Fan, S. Wen, X. Qing, G. Li, S. Li, W. Deng, *Energy Environ. Sci.* **2011**, *4*, 2062–2065; b) K. V. Rao, S. Mohapatra, T. Kumar Maji, S. J. George, *Chem. Eur. J.* **2012**, *18*, 4505–4509.
- [9] a) C. E. Chan-Thaw, A. Villa, P. Katekomol, D. Su, A. Thomas, *Nano Lett.* **2010**, *10*, 537–541; b) C. Xie, K. Wang, E. deKrat, W. Lin, *J. Am. Chem. Soc.* **2011**, *133*, 2056–2059; c) L. Chen, D. Jiang, *J. Am. Chem. Soc.* **2010**, *132*, 9138–9143.
- [10] a) T. Ben, H. Ren, S. Ma, D. Cao, J. Lan, X. Jing, W. Wang, J. Xu, F. Deng, J. M. Simmons, S. Qiu, G. Zhu, *Angew. Chem.* **2009**, *121*, 9621–9624; *Angew. Chem. Int. Ed.* **2009**, *48*, 9457–9460; b) D. Yuan, W. Lu, D. Zhao, H.-C. Zhou, *Adv. Mater.* **2011**, *23*, 3723–3725.
- [11] L. Chen, Y. Honsho, S. Seki, D. L. Jiang, *J. Am. Chem. Soc.* **2010**, *132*, 6742–6748.
- [12] a) A. Thomas, *Angew. Chem.* **2010**, *122*, 8506–8523; *Angew. Chem. Int. Ed.* **2010**, *49*, 8328–8344; b) R. Palkovits, M. Antonietti, P. Kuhn, A. Thomas, F. Schüth, *Angew. Chem.* **2009**, *121*, 7042–7045; *Angew. Chem. Int. Ed.* **2009**, *48*, 6909–6912; c) L. Chen, Y. Yang, Z. Guo, D. Jiang, *Adv. Mater.* **2011**, *23*, 3149–3154; d) D. S. Kundu, J. Schmidt, C. Bleschke, A. Thomas, S. Blechert, *Angew. Chem. Int. Ed.* **2012**, *51*, 5456–5459.
- [13] J. Boutagy, R. Thomas, *Chem. Rev.* **1974**, *74*, 87–99.

- [14] a) O. Mitsunobu, M. B. Yamada, *Bull. Chem. Soc. Jpn.* **1967**, *40*, 2380–2382; b) T. Mukaiyama, R. Matsueda, H. B. Maruyama, *Bull. Chem. Soc. Jpn.* **1970**, *43*, 1271.
- [15] a) Y. M. Kim, S. Yu, *J. Am. Chem. Soc.* **2003**, *125*, 1696–1697; b) S. Schweizer, J. Becht, C. L. Drian, *Tetrahedron* **2010**, *66*, 765–772.
- [16] a) T. Mukaiyama, M. Araki, H. Takei, *J. Am. Chem. Soc.* **1973**, *95*, 4763–4765; b) E. J. Corey, K. C. Nicolaou, *J. Am. Chem. Soc.* **1974**, *96*, 5614–5616; c) E. J. Corey, K. C. Nicolaou, L. S. Melvin, *J. Am. Chem. Soc.* **1975**, *97*, 653–654.
- [17] a) R. Appel, *Angew. Chem.* **1975**, *87*, 863–874; *Angew. Chem. Int. Ed. Engl.* **1975**, *14*, 801–811; b) J. G. Calzada, J. Hooz, *Org. Synth.* **1988**, *50-9*, 634–637.
- [18] a) H. Staudinger, J. Meyer, *Helv. Chim. Acta* **1919**, *2*, 635–646; b) Y. G. Gololobov, I. N. Zhmurova, L. F. Kasukhin, *Tetrahedron* **1981**, *37*, 437–472; c) E. F. V. Scriven, K. Turnbull, *Chem. Rev.* **1988**, *88*, 297–368; d) Y. G. Gololobov, L. F. Kasukhin, *Tetrahedron* **1992**, *48*, 1353–1406; e) S. Shah, J. D. Protasiewicz, *Coord. Chem. Rev.* **2000**, *210*, 181–201.
- [19] G. M. Scheuermann, L. Rumi, P. Steurer, W. Bannwarth, R. Mülhaupt, *J. Am. Chem. Soc.* **2009**, *131*, 8262–8270.
- [20] L. Wu, Z. W. Li, F. Zhang, Y. M. He, Q. H. Fan, *Adv. Synth. Catal.* **2008**, *350*, 846–862.
- [21] Z. Zheng, H. Li, T. Liu, R. Cao, *J. Catal.* **2010**, *270*, 268–274.
- [22] M. Dams, L. Drijkoningen, B. Pauwels, G. Tendeloo, D. E. Vos, P. A. Jacobs, *J. Catal.* **2002**, *209*, 225–236.
- [23] K. H. Shaughnessy, *Chem. Rev.* **2009**, *109*, 643–710.
- [24] Y. Zhang, S. N. Riduan, *Chem. Soc. Rev.* **2012**, *41*, 2083–2094.
- [25] Z. Wang, B. Zhang, H. Yu, G. Li, Y. Bao, *Soft Matter* **2011**, *7*, 5723–5730.
- [26] S. Ren, R. Dawson, J. Laybourn, X. Jiang, Y. Khimyak, D. J. Adams, A. I. Cooper, *Polym. Chem.* **2012**, *3*, 928–934.
- [27] K. S. W. Sing, D. H. Everett, R. A. W. Haul, L. Moscou, R. A. Pierotti, J. Rouqu  rol, T. Siemieniewska, *Pure Appl. Chem.* **1985**, *57*, 603–619.
- [28] Q. Chen, M. Luo, P. Hammershoj, D. Zhou, Y. Han, B. W. Laursen, C. G. Yan, B. H. Han, *J. Am. Chem. Soc.* **2012**, *134*, 6084–6087.
- [29] J. X. Jiang, A. Trewin, F. Su, C. D. Wood, H. Niu, J. T. A. Jones, Y. Z. Khimyak, A. I. Cooper, *Macromolecules* **2009**, *42*, 2658–2666.
- [30] P. Mohanty, L. D. Kull, K. Landskron, *Nat. Commun.* **2011**, *2*, 401.
- [31] A. Samanta, A. Zhao, G. K. H. Shimizu, P. Sarkar, R. Gupta, *Ind. Eng. Chem. Res.* **2012**, *51*, 1438–1463.
- [32] A. Torrisi, C. Mellot-Draznieks, R. G. Bell, *J. Chem. Phys.* **2010**, *132*, 044705.
- [33] H. Lim, M. C. Cha, J. Y. Chang, *Polym. Chem.* **2012**, *3*, 868–870.
- [34] a) A. Phan, C. J. Doonan, F. J. Uribe-Romo, C. B. Knobler, M. O’Keeffe, O. M. Yaghi, *Acc. Chem. Res.* **2010**, *43*, 58–67; b) R. Banerjee, H. Furukawa, D. Britt, C. Knobler, M. O’Keeffe, O. M. Yaghi, *J. Am. Chem. Soc.* **2009**, *131*, 3875–3877.
- [35] H. Furukawa, O. M. Yaghi, *J. Am. Chem. Soc.* **2009**, *131*, 8875–8883.
- [36] S. Ogasawara, S. Kato, *J. Am. Chem. Soc.* **2010**, *132*, 4608–4613.
- [37] a) S. B. Jang, *Tetrahedron Lett.* **1997**, *38*, 1793; b) I. Fenger, C. L. Drian, *Tetrahedron Lett.* **1998**, *39*, 4287–4290.
- [38] a) Y. Huang, Z. Zheng, T. Liu, J. L  , Z. Lin, H. Li, R. Cao, *Catal. Commun.* **2011**, *14*, 27; b) S. Li, J. Wang, Y. Kou, S. Zhang, *Chem. Eur. J.* **2010**, *16*, 1812–1818.

Received: January 29, 2013
Published online: June 14, 2013